

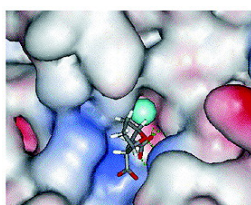
Article

Structure-Based Design of a Highly Selective Catalytic Site-Directed Inhibitor of Ser/Thr Protein Phosphatase 2B (Calcineurin)

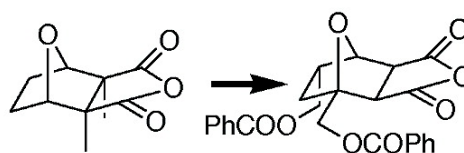
Yoshiyasu Baba, Nozomu Hirukawa, Naoto Tanohira, and Mikiko Sodeoka

J. Am. Chem. Soc., **2003**, 125 (32), 9740-9749 • DOI: 10.1021/ja034694y • Publication Date (Web): 22 July 2003

Downloaded from <http://pubs.acs.org> on March 29, 2009



PP2B catalytic site with "core" structure



Cantharidin

PP1, PP2A selective Inhibitor

PP2B selective Inhibitor

More About This Article

Additional resources and features associated with this article are available within the HTML version:

- Supporting Information
- Links to the 2 articles that cite this article, as of the time of this article download
- Access to high resolution figures
- Links to articles and content related to this article
- Copyright permission to reproduce figures and/or text from this article

[View the Full Text HTML](#)



ACS Publications
 High quality. High impact.

Structure-Based Design of a Highly Selective Catalytic Site-Directed Inhibitor of Ser/Thr Protein Phosphatase 2B (Calcineurin)

Yoshiyasu Baba,^{†,‡,§} Nozomu Hirukawa,^{†,‡} Naoto Tanohira,[‡] and Mikiko Sodeoka^{*,†,‡}

Contribution from the Institute of Multidisciplinary Research for Advanced Materials (IMRAM), Tohoku University, 2-1-1 Katahira, Aoba, Sendai, Miyagi 980-8577, Japan, and Sagami Chemical Research Center, Nishi-Ohnuma, Sagamihara Kanagawa 229-0012, Japan

Received February 17, 2003; E-mail: sodeoka@tagen.tohoku.ac.jp

Abstract: Protein serine/threonine phosphatases (PP1, PP2A and PP2B) play important roles in intracellular signal transductions. The immunosuppressant drugs FK506 and cyclosporin A (CsA) bind to immunophilins, and these complexes selectively inhibit PP2B (calcineurin), leading to the suppression of T-cell proliferation. Both FK506 and CsA must, however, form complexes with immunophilins to exert their inhibitory action on PP2B. Thus, it is of interest to find a direct and selective inhibitor of PP2B that does not involve the immunophilins as a biological tool for studies of PP2B and also as a candidate therapeutic agent. We selected the simple natural product cantharidin, a known PP2A-selective inhibitor, as a lead compound for this project. Primary SAR indicated that norcantharidin (7-oxabicyclo[2.2.1]heptane-2,3-dicarboxylic anhydride) inhibits not only PP1 and PP2A but also PP2B, and a binding model of norcantharidin carboxylate to the PP2B catalytic site was computationally constructed. Based on this binding model, we designed and synthesized several cantharidin derivatives. Among these compounds, 1,5-dibenzoyloxymethyl-substituted norcantharidin was found to inhibit PP2B without inhibiting PP1 or PP2A. To our knowledge, this is the first highly selective catalytic site-directed inhibitor of PP2B.

Introduction

The reversible phosphorylation of proteins catalyzed by protein kinase and phosphatase plays an important role in intracellular signal transductions, such as regulation of cell proliferation or differentiation.¹ Protein phosphatases can be divided into two classes according to the substrate specificity, that is, protein serine/threonine phosphatase (PP) and protein tyrosine phosphatase (PTP). Furthermore, PP is categorized into four major subtypes, PP1, PP2A, PP2B, and PP2C.^{1d} PP2B (calcineurin) is a calcium and calmodulin-regulated phosphatase which is a heterodimer composed of a catalytic subunit (CnA, 59 kDa) and a calcium/calmodulin-binding subunit (CnB, 19 kDa).² The catalytic subunit of CnA shares a high degree of amino acid identity with PP1 and PP2A. PP1 and PP2A inhibitors, such as okadaic acid, tautomycin, and microcystin-LR, are well-known as tumor promoters.³ In contrast, inhibition

of PP2B is known to cause suppression of T-lymphocyte activation. The therapeutic immunosuppressants FK506 and cyclosporin A form complexes with their binding proteins (FKBP and cyclophilin, respectively), and these complexes bind to CnB and inhibit its activity, leading to the suppression of T-cell proliferation.⁴ It is important to note that neither FK506 nor cyclosporin A alone can inhibit PP2B, and formation of the immunophilin complex is required for the PP2B inhibition. Recently, immunophilins have been shown to regulate the intracellular calcium ion channel or to be involved in various other biological processes.⁵ Some of the side effects of the above immunosuppressants may be caused by inhibition of the immunophilins. However, a direct and selective inhibitor of PP2B has not been reported so far. We started a project aiming at the development of a novel immunosuppressant, which binds the CnA catalytic site directly, without requiring immunophilins, to inhibit PP2B. In this paper, we describe the design and synthesis of highly selective catalytic site-directed inhibitors of PP2B.

The catalytic site structure of PPs is highly conserved (conserved amino acid sequence, GDXHG(X)_nGDXVDRG-(X)_nRGNHE) but is distinct from that of PTPs, which is characterized by the highly conserved loop structure, C(X)₅R.

[†] Tohoku University.

[‡] Sagami Chemical Research Center. This facility has moved and is currently at 2743-1 Hayakawa, Ayase, Kanagawa 252-1193, Japan.

[§] Present address: International Innovation Center, Kyoto University, Yoshida, Sakyo-ku, Kyoto 606-8501, Japan.

- (1) (a) Hunter, T. *Cell* **1995**, *80*, 225–236. (b) Taylor, W. P.; Widlanski, T. S. *Chem. Biol.* **1995**, *2*, 713–718. (c) Cohen, P.; Cohen, P. T. J. *Biol. Chem.* **1989**, *264*, 21435–21438. (d) Cohen, P. *Annu. Rev. Biochem.* **1989**, *58*, 453–508.
- (2) Klee, C. B.; Draetta, G. F.; Hubbard, M. J. *Adv. Enzymol. Relat. Areas Mol. Biol.* **1988**, *61*, 149–200.
- (3) (a) Takai, A.; Bialojan, C.; Troschka, M.; Ruegg, J. C. *FEBS Lett.* **1987**, *217*, 81–84. (b) MacKintosh, C.; Klumpp, S. *FEBS Lett.* **1990**, *277*, 137–140. (c) MacKintosh, C.; Beattie, K. A.; Klumpp, S.; Cohen, P.; Codd, G. A. *FEBS Lett.* **1990**, *264*, 187–192.

- (4) (a) Liu, J.; Farmer, J. D., Jr.; Lane W. S.; Friedman, J.; Weissman, I.; Schreiber, S. L. *Cell* **1991**, *66*, 807–815. (b) Schreiber, S. L.; Albers, M. W.; Brown, E. J. *Acc. Chem. Res.* **1993**, *26*, 412–420 and references cited therein.
- (5) Andreeva, L.; Heads, R.; Green, C. J. *Int. J. Exp. Pathol.* **1999**, *80*, 305–315.

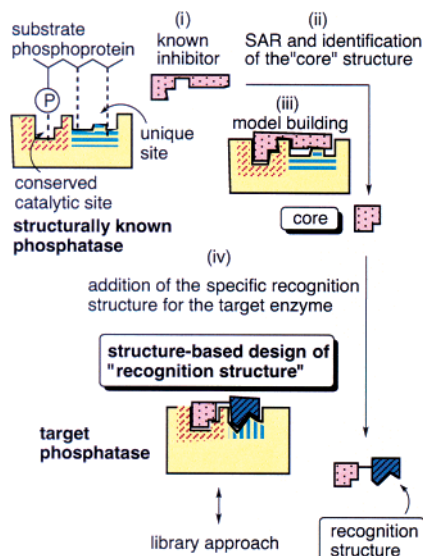


Figure 1. Strategy for the development of catalytic site-directed protein phosphatase inhibitors.

The conserved catalytic site interacts with phosphate oxygen atoms of the substrate, and each enzyme has a unique site surrounding the catalytic site that recognizes its specific substrate. Based on these general structural features of these enzymes, we designed a strategy for the development of selective protein phosphatase inhibitors. Briefly, (i) an enzyme in the same family as the target enzyme, which has a known tertiary structure, is selected, and a known inhibitor of the former enzyme is picked up as the lead compound for the target enzyme. (ii) Primary structure–activity relationships (SARs) between this inhibitor and the target enzyme are clarified, and a “core” structure that interacts with the highly conserved catalytic site is identified and optimized. (iii) A binding model of the “core” structure and the catalytic site of the enzyme is constructed by using computational docking techniques. (iv) Substituents which can interact with the unique regions of the target enzyme are introduced on to the “core” structure, based on the binding model.⁶ According to this strategy, we have identified a selective “core” structure which binds strongly to PTPs but not PPs. We found moderately selective inhibitors of several PTPs from a library of compounds having this “PTP core” structure.⁷ For the development of a highly selective inhibitor of PP2B, we decided to take a rational structure-based approach instead of the library approach (Figure 1).

The catalytic site structure is highly conserved among the major PPs (PP1, PP2A and PP2B), and two metal ions and coordinating and/or basic amino acid residues play a key role in the catalysis. The crystal structures of the PP1–microcystin complex⁸ and PP2B–FKBP–FK506 complex⁹ have been

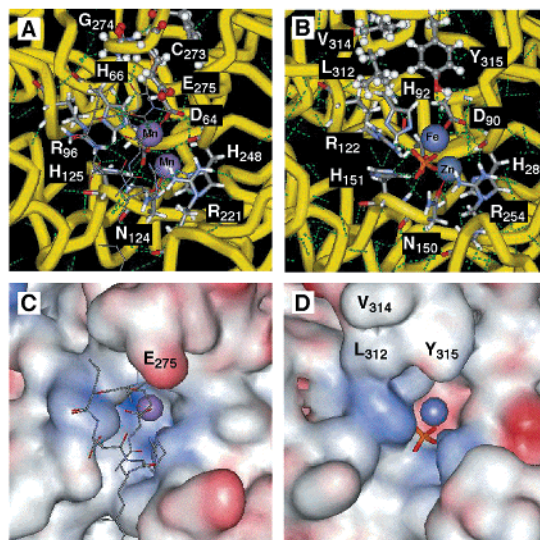


Figure 2. Crystal structures of PP1 and PP2B catalytic sites. (A) PP1–microcystin covalent complex (conserved residues are shown as sticks, unique residues are shown as ball-and-stick structures, and microcystin–LR is shown as a line). (B) PP2B–phosphate ion complex (conserved residues and phosphate anion are shown as sticks, and unique residues are shown as ball-and-stick structures). (C) PP1–microcystin covalent complex (solvent contact surface is shown). (D) PP2B–phosphate ion complex (solvent contact surface is shown).

reported. As shown in Figure 2, the catalytic sites are highly conserved. All amino acid residues act as metal ligands (D₉₀, H₉₂, D₁₁₈, N₁₅₀, H₁₉₉, H₂₈₁, PP2B numbering), and basic amino acid residues which interact with the phosphate group (R₁₂₂, H₁₅₁, R₂₅₄, PP2B numbering) are completely conserved. There are possible recognition sites near the catalytic site. A hydrophobic amino acid cluster is located near the upper ridge of the catalytic site in PP2B (L₃₁₂, V₃₁₄, Y₃₁₅). In contrast, there is a hydrophilic amino acid in the corresponding region of PP1 (C₂₇₃, G₂₇₄, E₂₇₅) and also PP2A (C₂₆₂, Y₂₆₃, R₂₆₄). The molecular topologies of these regions are also very different (Figure 2C and D).

Known PP1/PP2A inhibitors, including okadaic acid, microcystin-LR, tautomycin, calyculin A and cantharidin, have a variety of structures (Figure 3).^{3,10,11} These inhibitors contain a carboxylic acid, acid anhydride, or phosphate moiety, and it is likely that these functional groups mimic a phosphate group of the substrate phosphopeptide. The reported crystal structure of the PP1–microcystin complex reveals interaction between the carboxylic acids of microcystin and the basic amino acid residue in the catalytic site, in addition to the covalent bond with C₂₇₃ (Figure 2A). It is a substantial challenge to identify the “PP-selective core” structure in these PP1/PP2A-selective inhibitors and to create a PP2B-selective inhibitor by rational design based on the structural difference between PP1/PP2A and PP2B. Among these PP1/PP2A-selective inhibitors, we chose canthari-

(6) Approaches for increasing affinity to a target protein by tethering two individual fragments have already been successfully demonstrated. See: (a) Shuker, S. B.; Hajduk, P. J.; Meadows, R. P.; Fesik, S. W. *Science* **1996**, *274*, 1531–1534. (b) Mammen, M.; Choi, S.-K.; Whitesides, G. M. *Angew. Chem., Int. Ed.* **1998**, *37*, 2754–2794 and references therein. (7) (a) Sodeoka, M.; Sampe, R.; Kojima, S.; Baba, Y.; Usui, T.; Ueda, K.; Osada, H. *J. Med. Chem.* **2001**, *44*, 3216–3222. (b) Usui, T.; Kojima, S.; Kidokoro, S.; Ueda, K.; Osada, H.; Sodeoka, M. *Chem. Biol.* **2001**, *8*, 1209–1220. (c) Sodeoka, M.; Baba, Y. *Yuki Gosei Kagaku Kyokaiishi* **2001**, *59*, 1095–1102. (8) Goldberg, J.; Huang, H. B.; Kwon, Y. G.; Greengard, P.; Nairn, A. C.; Kuriyan, J. *Nature* **1995**, *376*, 745–753. Recently, the crystal structure of the PP1–calyculin complex was also reported. See: Kita, A.; Matsunaga, S.; Takai, A.; Kataiwa, H.; Wakimoto, T.; Fusetani, N.; Isobe, M.; Miki, K. *Structure* **2002**, *10*, 715–724.

(9) (a) Kissinger, C. R.; Perge, H. E.; Knighton, D. R.; Lewis, C. T.; Pelletier, L. A.; Tempczyk, A.; Kalish, V. J.; Tucker, K. D.; Showalter, R. E.; Moomaw, E. W.; Gastinel, L. N.; Habuka, N.; Chen, X.; Maldonado, F.; Barker, J. E.; Bacquet, R.; Villafranca, J. E. *Nature* **1995**, *378*, 641. (b) Griffith, J. P.; Kim, J. L.; Kim, E. E.; Sintchak, M. D.; Thomson, J. A.; Fitzgibbon, M. J.; Fleming, M. A.; Caron, P. R.; Hsiao, K.; Navia, M. A. *Cell* **1995**, *82*, 507–522. (10) Sheppeck, J. E.; Gauss, C.-M.; Chamberlin, A. R. *Bioorg. Med. Chem.* **1997**, *5*, 1739–1750 and references therein. (11) (a) Li, Y.-M.; Casida, J. E. *Proc. Natl. Acad. Sci. U.S.A.* **1992**, *89*, 11867–11870. (b) Li, Y.-M.; MacKintosh, C.; Casida, J. E. *Biochem. Pharmacol.* **1993**, *46*, 1435–1443. (c) Honkanen, R. E. *FEBS Lett.* **1993**, *330*, 283–286 and references therein.

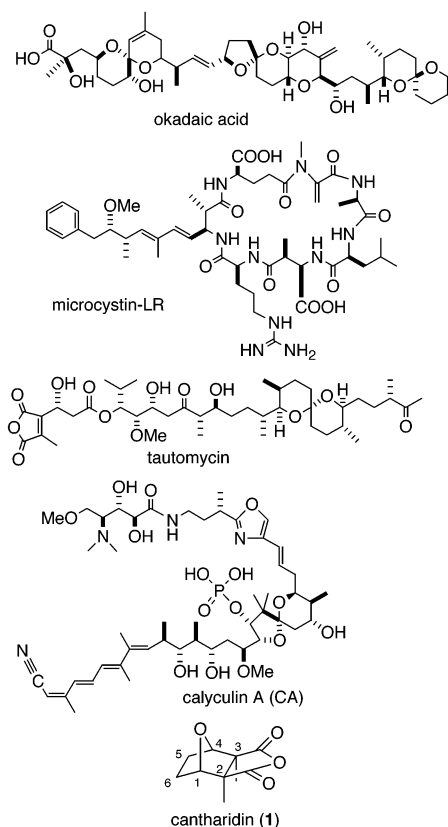


Figure 3. Naturally occurring Ser/Thr phosphatase inhibitors. Reported IC_{50} values for PPs are as follows:^{10,11c} (okadaic acid) PP1, 3 nM, PP2A, 0.2–1 nM, PP2B, >10 mM; (microcystin-LR) PP1, 0.1 nM, PP2A, 0.1 nM, PP2B, not determined; (tautomycin) PP1, 0.7 nM, PP2A, 0.7 nM, PP2B, ~70 mM; (calyculin A) PP1, 0.3–0.7 nM, PP2A, 0.2–1 nM, PP2B, >10 mM; (cantharidin) PP1, 1.7 μ M, PP2A, 0.16 μ M, PP2B, >1 mM.

cantharidin (1) as a lead compound. Cantharidin, an active constituent of the dried body of a Chinese blister beetle (*Mylabris phalerata* or *M. cichorii*), is a chemical defense material. The inhibitory activities of cantharidin on PP1 and PP2A (IC_{50} of sub μ M order) are much weaker¹¹ than those of other okadaic acid class compounds such as microcystin, tautomycin, and so forth (IC_{50} s of sub nM order),¹⁰ but we considered that the simple and rigid structure with an acid anhydride moiety was well suited as a lead for finding a good PP core. In fact, cantharidin was reported to inhibit PP2B very weakly (IC_{50} = 1 mM), although inhibition of PP2B by other okadaic acid class compounds was negligible.^{11c}

Results and Discussion

Basic SAR of Cantharidin Derivatives. Several reports on the SAR of cantharidin analogues as PP1/PP2A inhibitors have already been published,^{11,12} but there has been no systematic study comparing the inhibition of all three enzymes. We first

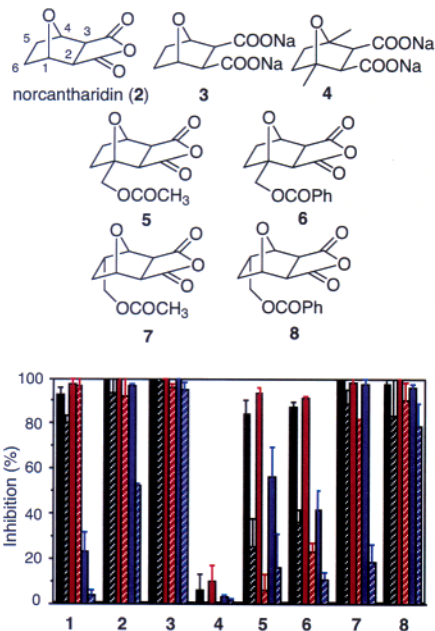


Figure 4. Basic structure–activity relationships of cantharidin derivatives 1–8. Black, red, and blue bars represent the inhibition of PP1, PP2A, and PP2B, respectively. Solid bars and striped bars indicate inhibition at 1 mM and 100 μ M drug concentrations, respectively.

examined the basic structure–activity relationship (SAR) of cantharidin analogues for PP1, PP2A, and PP2B (Figure 4).¹³ Several cantharidin analogues were tested for their inhibition of PP1, PP2A, and PP2B at concentrations of 1 mM and 100 μ M. As reported previously,^{11c} cantharidin (1) strongly inhibited PP1 and PP2A, but only a very weak inhibition of PP2B was observed. Norcantharidin (2), the analogue without the two methyl substituents at the C2 and C3 positions of cantharidin, showed a stronger inhibition of PP2B. Norcantharidic acid sodium salt (3) (endothal-sodium, a herbicide¹⁴) also inhibited all three PPs.¹⁵ It is likely that the dicarboxylic acid (salt) formed from the acid anhydride by hydrolysis under aqueous assay conditions is an active form, as observed in the case of tautomycin.¹⁶ We were pleased to find that 3 did not inhibit PTP-1B, a representative tyrosine phosphatase, even at >1 mM concentrations, indicating that this rigid norcantharidin dicarboxylate structure can be considered as the “PP-selective core”. Introduction of methyl groups at both the C1 and C4 positions (compound 4) almost abolished the inhibitory activity toward all phosphatases. We further synthesized the acid anhydride derivatives, because of the ease of synthesizing and handling these compounds, and examined their SAR. Compounds 5 and 6 having only one substituent at the bridgehead position also showed decreased inhibition of all PPs, but some inhibitory activity remained. The C1 substituent was more unfavorable in relation to PP1/PP2A than PP2B. A comparison of compounds 7 and 8 having a substituent at the C5-endo position was interesting. Compound 7, having an acetoxyethyl group,

(12) (a) McCluskey, A.; Taylor, C.; Quinn, R. J. *Bioorg. Med. Chem. Lett.* **1996**, *6*, 1025–1028. (b) Enz, A.; Zenke, G.; Pombo-Villar, E. *Bioorg. Med. Chem. Lett.* **1997**, *7*, 2513–2518. (c) McCluskey, A.; Keane, M. A.; Mudjee, L.-M.; Sim, A. T. R.; Sakoff, J.; Quinn, R. J. *Eur. J. Med. Chem.* **2000**, *35*, 957–964. (d) McCluskey, A.; Bowyer, M. C.; Collins, E.; Sim, A. T. R.; Sakoff, J. A.; Baldwin, M. L. *Bioorg. Med. Chem. Lett.* **2000**, *10*, 1687–1690. (e) McCluskey, A.; Walkom, C.; Bowyer, M. C.; Ackland, S. P.; Gardiner, E.; Sakoff, J. A. *Bioorg. Med. Chem. Lett.* **2001**, *11*, 2941–2946. (f) McCluskey, A.; Keane, M. A.; Walkom, C. C.; Bowyer, M. C.; Sim, A. T. R.; Young, D. J.; Sakoff, J. A. *Bioorg. Med. Chem. Lett.* **2002**, *12*, 391–393.

(13) Preliminary SAR results have already been reported; see: Sodeoka, M.; Baba, Y.; Kobayashi, S.; Hirukawa, N. *Bioorg. Med. Chem. Lett.* **1997**, *7*, 1833–1836.

(14) Matsuzawa, M.; Graziano, M. J.; Casida, J. E. *J. Agric. Food Chem.* **1987**, *35*, 823–829.

(15) Increased inhibition of PP2B by 1 and 2 has also been reported; see ref 11c.

(16) Sugiyama, Y.; Ohtani, I. I.; Isobe, M.; Takai, A.; Ubukata, M.; Isono, K. *Bioorg. Med. Chem. Lett.* **1996**, *6*, 3–8.

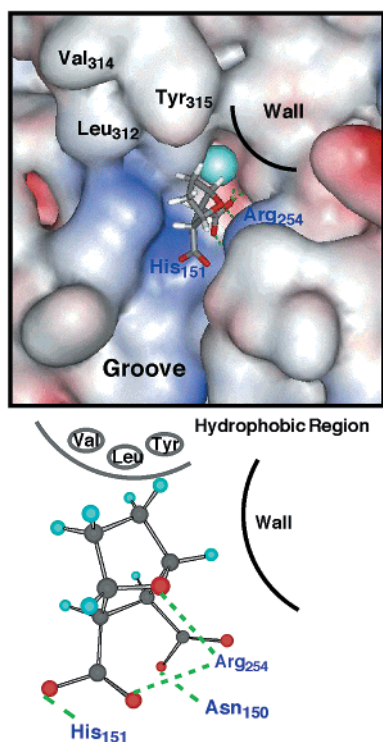


Figure 5. Proposed binding model of norcantharidin carboxylate to PP2B.

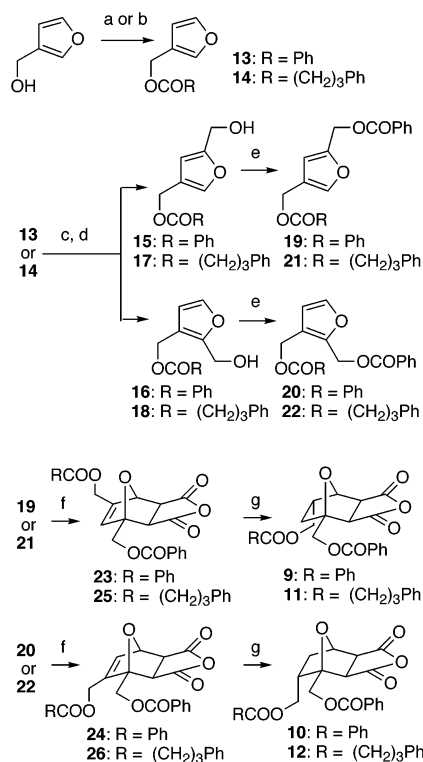
showed a slightly weakened inhibition of PP2B, whereas compound **8**, having a benzoyloxymethyl group, showed an increased inhibition of PP2B.¹⁷ These facts indicated that a hydrophobic group at this position interacts favorably with PP2B.

Computational Docking Model of PP2B and the “Core”.

We next constructed a binding model of the core structure to the PP2B catalytic site. To construct a binding model of norcantharidin carboxylate and the catalytic site of PP2B, a computational docking study was performed based on the reported PP2B–FKBP–FK506 complex structure. The preliminary binding model was constructed using the Affinity module of the Insight II molecular modeling program. The structures were then subjected to energy minimization. Figure 5 shows a possible energy-minimized docking model of norcantharidin dicarboxylate and PP2B. Interactions between phosphate oxygens, two metals (Fe, Zn), and amino acids (R₂₅₄, R₁₂₂, H₁₅₁) were observed in the crystal structure of the PP2B–phosphate complex (Figure 2B). In this model, the carboxylate moieties interact with this region as a phosphate mimic. The SAR indicated that introduction of two methyl groups at the C1 and C4 positions (**4**) completely abolished inhibitory activity toward all PPs. In contrast, monosubstituted compounds at this position (**5** and **6**) still retained some inhibitory activity. As shown in Figure 2C and D, a narrow and deep groove exists in the catalytic site of PP1 and PP2B, which is supposed to be the substrate recognition site of each enzyme. This groove ends at the phosphate-binding pocket, and there is no room around the dicarboxylate except in this direction. According to this model, the C1 substituent of **5** and **6** can be fitted into the groove. It is

(17) Tatlock et al. also reported that substitution of the 5-endo-hydrogen of norcantharidin by hydrophobic residues increased inhibition of PP2B; see: Tatlock, J. H.; Linton, M. A.; Hou, X. J.; Kissinger, C. R.; Pelletier, L. A.; Showalter, R. E.; Tempezyk, A.; Villafraña, J. E. *Bioorg. Med. Chem. Lett.* **1997**, *7*, 1007–1012.

Scheme 1. Preparation of Disubstituted Derivatives^a



^a (a) BzCl, Et₃N, DMAP, CH₂Cl₂; (b) Ph(CH₂)₃COOH, DCC, DMAP, THF; (c) DMF, POCl₃, then sat. NaHCO₃; (d) NaBH₃CN, THF–MeOH–AcOH; (e) BzCl, Et₃N, DMAP, CH₂Cl₂; (f) toluene, 23 °C; (g) H₂, 5% Rh/Al₂O₃, THF–Et₂O.

likely that several binding modes other than this model exist for this simple core structure, but the C1 substituent is expected to restrict the binding orientation in any of them. As a result, even a small group such as methyl at the C4 position might effectively prevent binding of **4** to all the enzymes. The observation that **8** showed stronger inhibition than **7** suggested an attractive interaction between the benzoyl group of **8** and hydrophobic residues of PP2B. All of the experimental results can be well explained by this model. To develop a PP2B-selective inhibitor, we next planned to synthesize 1,5- or 1,6-disubstituted derivatives based on this model. We expected that the C1 substituent would fix the binding orientation, and a hydrophobic substituent at the C5 or C6 position should have an attractive interaction with PP2B but a repulsive interaction with PP1/PP2A.

Disubstituted Cantharidin Derivatives. According to Scheme 1, we synthesized the disubstituted derivatives **9**–**12**. Disubstituted furan derivatives **19**–**22** were prepared by Vilsmeier reaction of 3-acyloxymethylfuran **13** and **14**. The mixture of formylated products was reduced with NaBH₃CN under an acidic condition (THF–acetic acid) to yield 2-hydroxymethyl-3-acyloxymethylfuran and 2-hydroxymethyl-4-acyloxymethylfuran without acyl transfer. The alcohols were treated with benzoyl chloride to give 2-benzoyloxymethyl-4-acyloxymethylfurans **19** and **21** and 2-benzoyloxymethyl-3-acyloxymethylfurans **20** and **22**. Diels–Alder reaction of the disubstituted furan derivatives with maleic anhydride proceeded at 23 °C in toluene to yield the corresponding adducts in a moderate yield. Hydrogenation of the resulting adducts by using a Rh/Al₂O₃ complex as a catalyst gave the desired 1,6- and 1,5-disubstituted

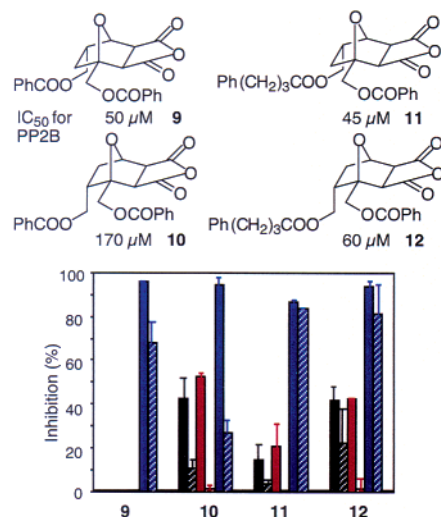


Figure 6. Inhibition of PP1, PP2A, and PP2B by disubstituted derivatives 9–12. Black, red, and blue bars represent the inhibition of PP1, PP2A, and PP2B, respectively. Solid bars and striped bars indicate inhibition at 1 mM and 100 μ M drug concentrations, respectively.

exo,exo-7-oxabicyclo[2.2.1]heptane-2,3-dicarboxylic anhydride derivatives 9–12.

The inhibitory activities for all PPs were examined. As expected, these compounds showed selective inhibition of PP2B. In particular, the 1,5-dibenzoyloxymethyl derivative 9 showed greatly increased inhibition of PP2B (IC_{50} = 50 μ M) compared to 6 (IC_{50} = > 1 mM) and no inhibition of PP1 or PP2A (Figure 6). It is likely that introduction of a large hydrophobic substituent at the C5 position not only increases the attractive interaction between 9 and hydrophobic residues of PP2B (AA_{312–314}) as expected but also effectively prevents the binding of 9 to PP1 and PP2A, probably through an unfavorable interaction between the rigid and hydrophobic residue at the C5 position and a hydrophilic amino acid residue (E₂₇₅ of PP1 and R₂₆₄ of PP2A). A more flexible 5-*endo*-phenylbutyroxymethyl derivative 11 (IC_{50} = 45 μ M) and 6-substituted derivatives 10 (IC_{50} = 170 μ M) and 12 (IC_{50} = 60 μ M) were less selective, suggesting that a substituent at the C6 position and a flexible substituent at the C5 position are less effective to block binding to PP1 and PP2A.

Figure 7 shows dose–response curves of phosphatase inhibition by compound 9 and known inhibitors. No inhibition of PP1 by 9 was observed over the range of concentration tested (5 μ M–1 mM), and PP2A inhibition by 9 was also negligible. Okadaic acid and cantharidin strongly inhibited these enzymes under the same assay conditions (Figure 7A and B). The cyclosporin A–cyclophilin complex and FK506–FKBP complex are known to be ineffective if *p*-nitrophenyl phosphate (pNPP) was used as a substrate.^{4a,18} In contrast to these regulatory site-directed inhibitors, 9 was effective even if this small substrate was used (Figure 6). To compare the inhibitory activity of 9 with that of a cyclosporin A–cyclophilin A complex, we next carried out PP2B inhibition assays using RII phosphopeptide¹⁸ as a substrate (Figure 7C). Compound 9 was effective for the inhibition of the PP2B-catalyzed phosphopeptide hydrolysis (IC_{50} = 7 μ M).

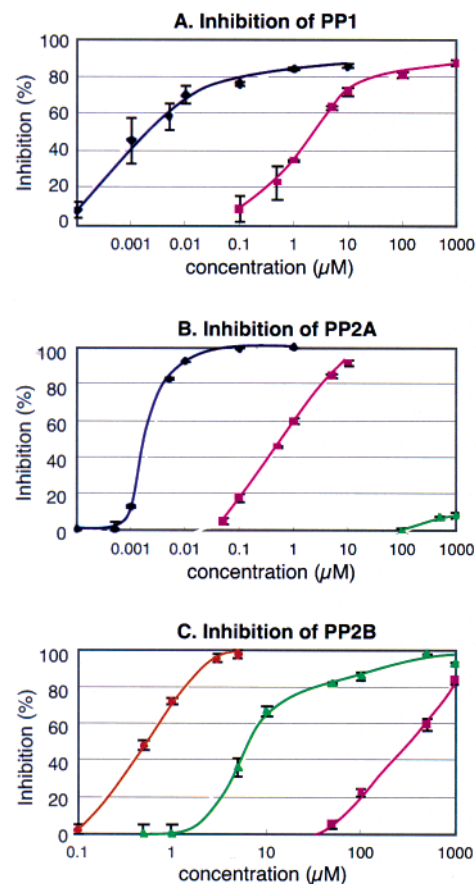


Figure 7. Inhibition of PP1, PP2A, and PP2B by okadaic acid, cantharidin, cyclosporin–cyclophilin complex, and 9. (A) Inhibition of PP1 by okadaic acid (blue), cantharidin (pink), and 9 (green, not shown on the graph). (B) Inhibition of PP2A by okadaic acid (blue), cantharidin (pink), and 9 (green). (C) Inhibition of PP2B by cyclophilin A–cyclosporin A complex (orange), cantharidin (pink), and 9 (green).

Conclusion

In conclusion, we have succeeded in developing a highly selective catalytic site-directed inhibitor of PP2B using a rational approach. Norcantharidin dicarboxylate was found to be a good “PP-selective core” structure which could interact with the highly conserved catalytic site of PPs but not that of PTPs. The basic SAR was clarified, and a binding model of the “core” and PP2B was constructed. Finally, the highly selective PP2B inhibitor 9 was designed and synthesized based on the binding model and the structural difference between PP2B and PP1. To our knowledge, *this is the first example of a specific inhibitor of PP2B which directly binds to the catalytic site.* Work to obtain a more potent PP2B inhibitor by fine-tuning of the structure is continuing. The successful example of a complete change of subtype specificity described here indicates the potency of our approach. The basic strategy shown in Figure 1 should be applicable not only for protein phosphatases but also for other families of proteins.

Experimental Section

General Methods. Infrared (IR) spectra were measured on a JASCO FT/IR-5300 spectrometer. ¹H and ¹³C NMR spectra were recorded on a Bruker AM-400 or AC-200P, AVANCE 500 NMR, or JEOL JNM-LA-400. Chemical shifts are reported downfield from tetramethylsilane (=0) for ¹H NMR. For ¹³C NMR, chemical shifts are reported in the scale relative to the solvent used as an internal reference. Mass spectra

(18) Swanson, S. K.-H.; Born, T.; Zydowsky, L. D.; Cho, H.; Chang, H. Y.; Walsh, C.; Rusnak, F. *Proc. Natl. Acad. Sci. U.S.A.* **1992**, *89*, 3741–3745.

(MS) were obtained with a Hitachi M-80B or JEOL JMS-AX500 using an electron-impact or chemical ionization method or with a JEOL JMS-GCmateII using a fast atom bombardment method. Column chromatography was performed with silica gel 60 (40–100 μm) purchased from Kanto Chemical Co. In general, reactions were carried out under anhydrous conditions in dry solvents under an argon atmosphere. Purity of the compounds obtained was determined to be more than 95% based on the ^1H NMR spectral analysis.

Synthesis of Cantharidin Derivatives. Compounds **1** and **4** were commercial products, and other compounds were synthesized as follows.

Norcantharidin (2).^{12c} To a solution of *exo*-3,6-epoxy-1,2,3,6-tetrahydrophthalic anhydride (392 mg, 2.36 mmol) in THF (20 mL) was added 10% Pd/C (100 mg), and the mixture was stirred at room temperature under a hydrogen atmosphere for 4 h. The reaction mixture was filtered through Celite and concentrated in vacuo to give **2** (425 mg, quant.) as colorless crystals. Mp 116–119 °C; IR (KBr, cm^{-1}) 1870, 1790, 1720, 1600, 1450; ^1H NMR (250 MHz, CDCl_3) δ 1.61 (dt, $J = 14.1, 3.4$ Hz, 2H), 1.87–1.90 (m, 2H), 3.15 (s, 2H), 5.02 (dd, $J = 3.4, 2.2$ Hz, 2H).

Norcantharidin Disodiumsalt (3).^{12c} To a solution of **2** (4.80 mg, 0.029 mmol) in THF (0.5 mL) was added 0.1 N sodium bicarbonate in water (57.1 μL , 0.058 mmol). The mixture was stirred at room temperature for 1 h and concentrated in vacuo to give **3** (6.67 mg, quant.) as a white solid. ^1H NMR (400 MHz, D_2O) δ 1.37 (m, 2H), 1.49 (m, 2H), 2.69 (s, 2H), 4.55 (brs, 2H).

1-Acetoxyethyl-7-oxabicyclo[2.2.1]heptane-2,3-dicarboxylic Anhydride (5). To a solution of furfuryl alcohol (4.91 g, 50.1 mmol) and Et_3N (20.9 mL, 150 mmol) in dichloromethane (25 mL) was added acetic anhydride (10.2 g, 100 mmol), and the mixture was stirred at room temperature for 19 h. The reaction was quenched with saturated ammonium chloride, and the mixture was extracted with dichloromethane. The organic layer was washed with water and brine, dried over anhydrous Na_2SO_4 , and concentrated in vacuo. The crude product was purified by silica gel column chromatography (10:1 hexane/EtOAc) to give 2-acetoxyethylfuran (6.40 g, 91%) as a yellow oil. ^1H NMR (200 MHz, CDCl_3) δ 2.07 (s, 3H), 5.05 (s, 2H), 6.36 (dd, $J = 3.2, 1.8$ Hz, 1H), 6.41 (brd, $J = 3.2$ Hz, 1H), 7.42 (dd, $J = 1.8, 0.8$ Hz, 1H); ^{13}C NMR (100 MHz, CDCl_3) δ 20.9, 58.0, 110.5, 110.6, 143.3, 149.4, 170.6. HRMS (FAB, m/z) calcd for $\text{C}_7\text{H}_8\text{O}_3$, 140.0473; found, 140.0474.

A solution of 2-acetoxyethylfuran (700 mg, 5.00 mmol) and maleic anhydride (491 mg, 5.00 mmol) in toluene (5 mL) was stirred at room temperature for 97 h. The reaction mixture was filtered, washed with hexane–EtOAc (1:1 v/v), and dried in vacuo to give 1-acetoxyethyl-7-oxabicyclo[2.2.1]hept-5-ene-2,3-dicarboxylic anhydride (880 mg, 74%) as colorless crystals. Mp 113–115 °C; IR (KBr, cm^{-1}) 1740, 1660, 1380, 1040, 1090; ^1H NMR (400 MHz, CDCl_3) δ 2.13 (s, 3H), 3.23 (d, $J = 6.8$ Hz, 1H), 3.35 (d, $J = 6.8$ Hz, 1H), 4.55 (d, $J = 12.8$ Hz, 1H), 4.92 (d, $J = 12.8$ Hz, 1H), 5.46 (d, $J = 1.6$ Hz, 1H), 6.48 (d, $J = 5.7$ Hz, 1H), 6.64 (dd, $J = 5.7, 1.6$ Hz, 1H); ^{13}C NMR (100 MHz, CDCl_3) δ 20.6, 49.6, 51.3, 60.7, 82.2, 90.7, 137.4, 138.0, 167.8, 169.3, 170.3. LRMS (EI, m/z) 239 ($\text{M}^+ + 1$).

To a solution of 1-acetoxyethyl-7-oxabicyclo[2.2.1]hept-5-ene-2,3-dicarboxylic anhydride (28.3 mg, 0.12 mmol) in THF (2 mL) was added 10% Pd/C (5 mg), and the mixture was stirred at room temperature under a hydrogen atmosphere for 4 h. The reaction mixture was filtered through Celite and concentrated in vacuo to give **5** (28.5 mg, quant.) as colorless crystals. Mp 125–129 °C; IR (KBr, cm^{-1}) 2960, 1740, 1370; ^1H NMR (400 MHz, CDCl_3) δ 1.64–1.78 (m, 2H), 1.87 (ddd, $J = 12.5, 11.8, 3.4$ Hz, 1H), 2.02–2.10 (m, 1H), 2.12 (s, 3H), 3.24 (d, $J = 7.5$ Hz, 1H), 3.34 (d, $J = 7.5$ Hz, 1H), 4.54 (d, $J = 12.5$ Hz, 1H), 4.62 (d, $J = 12.5$ Hz, 1H), 5.05 (d, $J = 5.3$ Hz, 1H); ^{13}C NMR (100 MHz, CDCl_3) δ 20.6, 29.2, 31.0, 51.3, 51.8, 61.9, 80.1, 87.3, 168.9, 170.2, 170.7. HRMS (FAB, m/z) calcd for $\text{C}_{11}\text{H}_{12}\text{O}_6$, 240.0634; found, 240.0623.

1-Benzoyloxymethyl-7-oxabicyclo[2.2.1]heptane-2,3-dicarboxylic Anhydride (6). To a solution of furfuryl alcohol (1.00 g, 10.2 mmol)

in dry pyridine (10 mL) was added benzoyl chloride (2.15 g, 15.3 mmol) at room temperature. The mixture was stirred for 3 h and then acidified with 1 N HCl (5 mL). After neutralization with saturated aqueous sodium bicarbonate, the mixture was extracted with EtOAc, and the organic layer was washed with water and brine, dried over anhydrous MgSO_4 , and concentrated in vacuo. The crude product was purified by silica gel column chromatography (20:1 hexane/EtOAc) to give 2-benzoyloxymethylfuran (647 mg, 31%) as a colorless oil. IR (neat, cm^{-1}) 1720, 1600, 1580, 1500, 1370, 1310, 1280; ^1H NMR (400 MHz, CDCl_3) δ 5.24 (s, 2H), 6.51 (dd, $J = 1.7, 1.7$ Hz, 1H), 7.41–7.46 (m, 3H), 7.53–7.59 (m, 2H), 8.02–8.08 (m, 2H); ^{13}C NMR (100 MHz, CDCl_3) δ 58.2, 110.6, 120.5, 128.3, 129.6, 130.1, 133.0, 141.6, 143.4, 166.4; LRMS (EI, m/z) 202 (M^+), 105, 81. HRMS (FAB, m/z) calcd for $\text{C}_{12}\text{H}_{10}\text{O}_3$, 202.0630; found, 202.0631.

A solution of 2-benzoyloxymethylfuran (647 mg, 3.12 mmol) and maleic anhydride (314 mg, 3.12 mmol) in toluene (5 mL) was stirred at 80 °C for 456 h. The reaction mixture was cooled to room temperature, and the crude product was collected by filtration and washed with hexane to afford 1-benzoyloxymethyl-7-oxabicyclo[2.2.1]hept-5-ene-2,3-dicarboxylic anhydride (437 mg, 46%) as colorless crystals. Mp 152–154 °C; IR (KBr, cm^{-1}) 3020, 1860, 1790, 1720, 1600, 1450; ^1H NMR (250 MHz, CDCl_3) δ 3.30 (d, $J = 6.9$ Hz, 1H), 3.37 (d, $J = 6.9$ Hz, 1H), 4.81 (d, $J = 13.0$ Hz, 1H), 5.20 (d, $J = 13.0$ Hz, 1H), 5.48 (d, $J = 1.5$ Hz, 1H), 6.53–6.65 (m, 2H), 7.40–7.63 (m, 3H), 8.02–8.07 (m, 2H); ^{13}C NMR (125 MHz, CDCl_3) δ 49.3, 50.9, 60.6, 81.8, 90.5, 128.0, 128.8, 129.4, 133.0, 137.1, 137.6, 165.4, 167.4, 168.9; LRMS (EI, m/z) 301 ($\text{M}^+ + 1$), 283, 203; Anal. Calcd for $\text{C}_{16}\text{H}_{12}\text{O}_6$: C, 64.00; H, 4.03. Found: C, 63.92; H, 4.01.

To a solution of 1-benzoyloxymethyl-7-oxabicyclo[2.2.1]hept-5-ene-2,3-dicarboxylic anhydride (96.3 mg, 0.32 mmol) in THF (5 mL) was added 10% Pd/C (20 mg), and the mixture was stirred at room temperature under a hydrogen atmosphere for 18 h. The reaction mixture was filtered through Celite and concentrated in vacuo. The crude product was purified by silica gel column chromatography (EtOAc) and recrystallized with 2-propanol to give **6** (51.0 mg, 53%) as colorless crystals. Mp 109–110 °C; IR (KBr, cm^{-1}) 1870, 1790, 1720, 1600, 1450; ^1H NMR (250 MHz, CDCl_3) δ 1.68–1.83 (m, 2H), 1.92–2.20 (m, 2H), 3.32 (d, $J = 7.5$ Hz, 1H), 3.36 (d, $J = 7.5$ Hz, 1H), 4.79 (d, $J = 12.5$ Hz, 1H), 4.94 (d, $J = 12.5$ Hz, 1H), 5.08 (d, $J = 5.0$ Hz, 1H), 7.39–7.60 (3H, m), 8.03–8.07 (m, 2H); ^{13}C NMR (125 MHz, CDCl_3) δ 29.2, 31.2, 51.5, 51.9, 62.3, 80.1, 87.6, 128.5, 129.4, 129.8, 133.3, 165.7, 169.0, 170.8; LRMS (CI, m/z) 303 ($\text{M}^+ + 1$), 181, 105. Anal. Calcd for $\text{C}_{16}\text{H}_{14}\text{O}_6$: C, 63.57; H, 4.67. Found: C, 63.37; H, 4.65.

5-Acetoxyethyl-7-oxabicyclo[2.2.1]heptane-2,3-dicarboxylic Anhydride (7). To a solution of 3-furanmethanol (1.02 g, 3.72 mmol) and Et_3N (1.04 mL, 7.44 mmol) in dichloromethane (30 mL) was added acetic anhydride (573 mL, 4.09 mmol), and the mixture was stirred at room temperature for 30 h. The reaction was quenched with saturated ammonium chloride, and the mixture was extracted with dichloromethane. The organic layer was washed with water and brine, dried over anhydrous Na_2SO_4 , and concentrated in vacuo. The crude product was purified by silica gel column chromatography (dichloromethane) to give 3-furylmethyl acetate (711 mg, quant.) as a colorless oil. ^1H NMR (200 MHz, CDCl_3) δ 2.07 (s, 3H), 4.98 (s, 2H), 6.43 (d, $J = 1.3$ Hz, 1H), 7.40 (d, $J = 1.3$ Hz, 1H), 7.47 (brs, 1H); ^{13}C NMR (100 MHz, CDCl_3) δ 21.0, 57.7, 110.6, 120.3, 141.6, 143.4, 170.9; LRMS (EI, m/z) 140 (M^+). HRMS (FAB, m/z) calcd for $\text{C}_7\text{H}_8\text{O}_3$, 140.0473; found, 140.0468.

A solution of 3-furylmethyl acetate (695 mg, 4.96 mmol) and maleic anhydride (486 mg, 4.96 mmol) in toluene (3 mL) was stirred at room temperature for 117 h. The reaction mixture was filtered and dried in vacuo to give 5-acetoxyethyl-7-oxabicyclo[2.2.1]hept-5-ene-2,3-dicarboxylic anhydride (961 mg, 81%) as colorless crystals. Mp 112–116 °C; IR (KBr, cm^{-1}) 2960, 1780, 1740, 1650, 1370, 1040, 1090; ^1H NMR (400 MHz, CDCl_3) δ 2.12 (s, 3H), 3.23 (d, $J = 6.9$ Hz, 1H),

3.29 (d, $J = 6.9$ Hz, 1H), 4.75 (dd, $J = 14.5, 1.7$ Hz, 1H), 4.80 (dd, $J = 14.5, 1.4$ Hz, 1H), 5.36 (s, 1H), 5.45 (d, $J = 1.4$ Hz, 1H), 6.38 (ddd, $J = 1.7, 1.4, 1.4$ Hz, 1H). ^{13}C NMR (100 MHz, CDCl_3) δ 20.7, 48.4, 49.6, 59.0, 82.8, 82.9, 132.6, 147.0, 169.6, 169.8, 170.5.

To a solution of 5-acetoxymethyl-7-oxabicyclo[2.2.1]hept-5-ene-2,3-dicarboxylic anhydride (119 mg, 0.50 mmol) in THF (5 mL) was added 10% Pd/C (25 mg). The mixture was stirred at room temperature under a hydrogen atmosphere for 3 h, filtered through Celite, and concentrated in vacuo to give **7** (105 mg, 88%) as colorless crystals. Mp 94–97 °C; IR (KBr, cm^{-1}) 2960, 1760, 1690, 1370, 1280, 1240; ^1H NMR (400 MHz, CDCl_3) δ 1.21 (dd, $J = 12.7$ Hz, 5.4 Hz, 1H), 2.11 (s, 3H), 2.17 (dd, $J = 12.7, 5.6$ Hz, 1H), 2.64 (m, 1H), 3.14 (d, $J = 7.4$ Hz, 1H), 3.50 (d, $J = 7.4$ Hz, 1H), 3.96 (dd, $J = 11.7$ Hz, 9.8 Hz, 1H), 4.26 (dd, $J = 11.7$ Hz, 5.6 Hz, 1H), 4.98 (d, 5.6 Hz, 1H), 5.01 (d, 4.9 Hz, 1H); ^{13}C NMR (100 MHz, CDCl_3) δ 20.8, 31.7, 39.4, 46.0, 50.5, 63.3, 80.6, 82.1, 170.8, 170.9, 171.6. HRMS (FAB, m/z) calcd for $\text{C}_{11}\text{H}_{12}\text{O}_6 + \text{H}^+$, 241.0712; found, 241.0717.

3-Furylmethyl Benzoate (13). To a solution of 3-furanmethanol (1.09 g, 11.1 mmol) in dry pyridine (10 mL) was added benzoyl chloride (2.35 g, 16.7 mmol) at room temperature. The reaction mixture was stirred for 3 h, acidified with 1 N HCl (5 mL), neutralized with saturated aqueous sodium bicarbonate, and extracted with Et_2O . The organic layer was washed with water and brine, dried over anhydrous MgSO_4 , and concentrated in vacuo. The crude product was purified by silica gel column chromatography (20:1 hexane/EtOAc) to give **13** (2.22 g, 97%) as a colorless oil. IR (neat, cm^{-1}) 1720, 1600, 1580, 1500, 1370, 1310, 1280; ^1H NMR (400 MHz, CDCl_3) δ 5.24 (s, 2H), 6.51 (dd, $J = 1.7, 1.7$ Hz, 1H), 7.41–7.46 (m, 3H), 7.53–7.59 (m, 2H), 8.02–8.08 (m, 2H); ^{13}C NMR (100 MHz, CDCl_3) δ 58.2, 110.6, 120.5, 128.3, 129.6, 130.1, 133.0, 141.6, 143.4, 166.4; LRMS (EI, m/z) 202 (M^+), 105, 81. HRMS (FAB, m/z) calcd for $\text{C}_{12}\text{H}_{10}\text{O}_3$, 202.0630; found, 202.0618.

5-Benzoyloxymethyl-7-oxabicyclo[2.2.1]heptane-2,3-dicarboxylic Anhydride (8). A solution of **13** (1.05 g, 5.25 mmol) and maleic anhydride (477 mg, 4.87 mmol) in toluene (5 mL) was stirred at 80 °C for 14 h. The reaction mixture was cooled at room temperature, and then the product was collected by filtration, washed with benzene, and dried in vacuo to give 5-benzoyloxymethyl-7-oxabicyclo[2.2.1]hept-5-ene-2,3-dicarboxylic anhydride (1.29 g, 89%) as a white solid. Mp, 134–137 °C; IR (KBr, cm^{-1}) 1860, 1790, 1720, 1600, 1580, 1490, 1450, 1310, 1270; ^1H NMR (400 MHz, CDCl_3) δ 3.25 (d, $J = 6.9$ Hz, 1H), 3.37 (d, $J = 6.9$ Hz, 1H), 5.04 (d, $J = 1.5$ Hz, 2H), 5.45 (s, 1H), 5.47 (d, $J = 1.3$ Hz, 1H), 6.45 (m, 1H), 7.45–7.51 (m, 3H), 8.02–8.06 (m, 2H); ^{13}C NMR (100 MHz, CDCl_3) δ 48.7, 50.0, 59.9, 81.9, 82.3, 128.7, 129.2, 132.7, 133.5, 146.1, 165.3, 171.2, 171.3; LRMS (EI, m/z) 301 ($\text{M}^+ + 1$), 202, 105. Anal. Calcd for $\text{C}_{16}\text{H}_{12}\text{O}_6$: C, 64.00; H, 4.03. Found: C, 63.86; H, 3.84.

To a solution of 5-benzoyloxymethyl-7-oxabicyclo[2.2.1]hept-5-ene-2,3-dicarboxylic anhydride (199 mg, 0.66 mmol) in THF (5 mL) was added 10% Pd/C (20 mg), and the mixture was stirred at room temperature under a hydrogen atmosphere for 3 h. The reaction mixture was filtered through Celite and concentrated in vacuo. The crude product was recrystallized with 2-propanol to give **8** (133 mg, 67%) as colorless crystals. Mp 145–149 °C; IR (KBr, cm^{-1}) 1860, 1840, 1780, 1710, 1600, 1590, 1470, 1450, 1390, 1320, 1290; ^1H NMR (200 MHz, CDCl_3) δ 1.32 (dd, $J = 12.7, 5.4$ Hz, 1H), 2.22 (ddd, $J = 12.7, 12.7, 5.7$ Hz, 1H), 2.72–2.87 (m, 1H), 3.20 (d, $J = 7.5$ Hz, 1H), 3.61 (d, $J = 7.5$ Hz, 1H), 4.21 (dd, $J = 11.8, 9.5$ Hz, 1H), 4.55 (dd, $J = 11.8, 5.7$ Hz, 1H), 5.06 (d, $J = 5.5$ Hz, 1H), 5.08 (d, $J = 4.7$ Hz, 1H), 7.43–7.67 (m, 3H), 8.00–8.07 (m, 2H); ^{13}C NMR (125 MHz, CDCl_3) δ 31.8, 39.7, 46.1, 50.6, 63.7, 128.7, 129.3, 129.6, 133.6, 166.2, 170.8, 171.4; LRMS (CI, m/z) 303 ($\text{M}^+ + 1$), 180, 105. Anal. Calcd for $\text{C}_{16}\text{H}_{14}\text{O}_6$: C, 63.57; H, 4.67. Found: C, 63.50; H, 4.53.

3-Furylmethyl-4-phenylbutanoate (14). To a solution of 3-furanmethanol (2.04 g, 20.7 mmol) in dry THF (20 mL) was added 4-phenylbutyric acid (3.24 g, 19.7 mmol), DCC (8.56 g, 41.5 mg), and DMAP (1.25 g, 10.4 mmol) at room temperature, and the mixture was

stirred for 27 h. The reaction mixture was filtered through Celite, and 1 N HCl (5 mL) was added. The mixture was diluted with EtOAc (10 mL), washed with saturated aqueous sodium bicarbonate, water, and brine, dried over anhydrous MgSO_4 , and concentrated in vacuo. The crude product was purified by silica gel column chromatography (3:1 hexane/EtOAc) to give **14** (3.48 g, 69%) as a colorless oil. IR (neat, cm^{-1}) 2926, 2853, 1740, 1600, 1500, 1480, 1430, 1140, 1040; ^1H NMR (250 MHz, CDCl_3) δ 1.96 (tt, $J = 7.5, 7.5$ Hz, 2H), 2.34 (t, $J = 7.5$ Hz, 2H), 2.64 (t, $J = 7.5$ Hz, 2H), 4.98 (s, 2H), 6.42 (d, $J = 1.3$ Hz, 1H), 7.17–7.47 (m, 7H); ^{13}C NMR (125 MHz, CDCl_3) δ 26.5, 33.6, 35.1, 57.6, 110.5, 120.5, 126.0, 128.4, 128.5, 141.3, 141.5, 143.4, 173.3; LRMS (EI, m/z) 244 (M^+), 163, 117, 81. HRMS (FAB, m/z) calcd for $\text{C}_{15}\text{H}_{16}\text{O}_3$, 244.1100; found, 244.1093.

4-Benzoyloxymethyl-2-hydroxymethylfuran (15) and 3-Benzoyloxymethyl-2-hydroxymethylfuran (16). A mixture of DMF (3.00 g, 41.1 mmol) and phosphorus oxychloride (6.31 g, 41.1 mmol) was stirred at 0 °C for 1 h to give a Vilsmeier reagent. To the Vilsmeier reagent was slowly added **13** (5.55 g, 27.4 mmol) at 0 °C, and stirring was continued for 1.5 h. After the resulting mixture was warmed to room temperature over 20 h, it was poured into saturated aqueous sodium bicarbonate (100 mL) and stirring was continued for 2.5 h. The reaction mixture was extracted with Et_2O , and the organic layer was washed with water and brine, dried over anhydrous MgSO_4 , and concentrated in vacuo. The crude product was purified by silica gel column chromatography (8:1 hexane/EtOAc) to give a 1:3 mixture of 4-benzoyloxymethyl-2-formylfuran and 3-benzoyloxymethyl-2-formylfuran (5.61 g, 89%) as a colorless oil.

To a solution of 4-benzoyloxymethyl-2-formylfuran and 3-benzoyloxymethyl-2-formylfuran (5.61 g, 24.4 mmol) in a mixture of methanol (55 mL), dry THF (55 mL), and acetic acid (2.7 mL) was added NaBH_3CN (2.30 g, 36.6 mmol) at room temperature. The mixture was stirred for 2 h and then diluted with EtOAc (170 mL), washed with saturated aqueous sodium bicarbonate, water, and brine, dried over anhydrous MgSO_4 , and concentrated in vacuo. The crude product was purified by silica gel column chromatography (4:1 hexane/EtOAc) to give **15** (0.98 g, 19%) as a yellow oil and **16** (2.84 g, 57%) as a colorless solid. **15:** IR (neat, cm^{-1}) 3370, 2950, 1720, 1610, 1460, 1280, 1280, 1110; ^1H NMR (500 MHz, CDCl_3) δ 1.94 (s, 1H), 4.59 (s, 2H), 5.19 (s, 2H), 6.42 (s, 1H), 7.42–7.45 (m, 2H), 7.51 (s, 1H), 7.54–7.57 (m, 1H), 8.03–8.05 (m, 2H); ^{13}C NMR (125 MHz, CDCl_3) δ 57.5, 58.2, 108.8, 121.3, 128.3, 129.6, 130.0, 133.0, 141.5, 155.0, 166.5; Mass (EI, m/z) 232 (M^+), 110, 105. HRMS (EI, m/z) calcd for $\text{C}_{20}\text{H}_{16}\text{O}_5$, 232.0736; found, 232.0758. **16:** mp, 66–67 °C; IR (KBr, cm^{-1}) 3370, 2950, 1720, 1610, 1460, 1280, 1280, 1110; ^1H NMR (250 MHz, CDCl_3) δ 2.75 (s, 1H), 4.75 (s, 2H), 5.27 (s, 2H), 6.46 (d, $J = 1.8$ Hz, 1H), 7.36 (d, $J = 1.8$ Hz, 1H), 7.41–7.44 (m, 2H), 7.54–7.57 (m, 1H), 8.01–8.03 (m, 2H); ^{13}C NMR (125 MHz, CDCl_3) δ 55.5, 58.1, 111.7, 117.0, 128.4, 129.7, 130.0, 133.2, 142.2, 152.9, 167.0; LRMS (EI, m/z) 232 (M^+), 110, 105. HRMS (EI, m/z) calcd for $\text{C}_{20}\text{H}_{16}\text{O}_5$, 232.0736; found, 232.0750.

2-Hydroxymethyl-4-(4-phenylbutanoyloxymethyl)furan (17) and 2-Hydroxymethyl-3-(4-phenylbutanoyloxymethyl)furan (18). A mixture of DMF (1.14 mL, 41.7 mmol) and phosphorus oxychloride (1.48 g, 14.7 mmol) was stirred at 0 °C for 30 min to give a Vilsmeier reagent. To the Vilsmeier reagent was slowly added **14** (1.80 g, 7.37 mmol) at 0 °C, and the reaction mixture was stirred for 30 min. After the reaction mixture was warmed to room temperature, the reaction mixture was further stirred for 70 h and then poured into saturated aqueous sodium bicarbonate (30 mL) at 0 °C, and stirring was continued for 4 h. The reaction mixture was extracted with Et_2O , and the organic layer was washed with water and brine, dried over anhydrous MgSO_4 , and concentrated in vacuo. The crude product was purified by silica gel column chromatography (7:1 hexane/EtOAc) to give 2-formyl-3-(4-phenylbutanoyloxymethyl)furan (1.48 g, 74%) and 2-formyl-4-(4-phenylbutanoyloxymethyl)furan (503 mg, 25%), each as a colorless oil. 2-Formyl-3-(4-phenylbutanoyloxymethyl)furan: IR (neat, cm^{-1})

2926, 2853, 1740, 1670, 1600, 1480, 1450, 1430, 1270, 1140; ^1H NMR (250 MHz, CDCl_3) δ 1.98 (tt, $J = 7.5, 7.5$ Hz, 2H), 2.39 (t, $J = 7.5$ Hz, 2H), 2.66 (t, $J = 7.5$ Hz, 2H), 5.33 (s, 2H), 6.61 (d, $J = 1.5$ Hz, 1H), 7.17–7.28 (m, 5H), 7.60 (d, $J = 1.5$ Hz, 1H), 9.85 (s, 1H). ^{13}C NMR (125 MHz, CDCl_3) δ 26.3, 33.3, 35.0, 56.9, 113.4, 126.0, 128.4, 128.4, 130.9, 141.1, 147.2, 148.5, 172.9, 178.7; LRMS (CI, m/z) 273 ($\text{M}^+ + 1$), 255, 163, 109, 91. 2-Formyl-4-(4-phenylbutanoyloxymethyl)-furan: IR (neat, cm^{-1}) 2820, 1740, 1670, 1600, 1520, 1450, 1270, 1140; ^1H NMR (250 MHz, CDCl_3) δ 1.93 (tt, $J = 7.5, 7.5$ Hz, 2H), 2.35 (t, $J = 7.5$ Hz, 2H), 2.64 (t, $J = 7.5$ Hz, 2H), 5.00 (s, 2H), 7.14–7.31 (m, 6H), 7.70 (s, 1H), 9.63 (s, 1H); ^{13}C NMR (125 MHz, CDCl_3) δ 26.3, 33.4, 35.0, 56.7, 120.9, 123.5, 126.0, 128.4, 128.4, 141.1, 146.7, 153.2, 173.1, 177.8; LRMS (EI, m/z) 272 (M^+), 255, 163, 109, 91.

To a solution of 2-formyl-4-(4-phenylbutanoyloxymethyl)furan (390 mg, 1.43 mmol) in methanol–THF–acetic acid (17.5 mL, 20:20:1 v/v) was added NaBH_3CN (225 mg, 3.58 mmol) at 0 °C. The mixture was stirred for 23 h at room temperature, then poured into saturated aqueous sodium bicarbonate (3 mL) at 0 °C, and extracted with EtOAc. The organic layer was washed with water and brine, dried over anhydrous MgSO_4 , and concentrated in vacuo. The crude product was purified by silica gel column chromatography (3:1 hexane/EtOAc) to give **17** (287 mg, 73%) as a colorless oil. IR (neat, cm^{-1}) 3450, 2940, 2853, 1740, 1500, 1460, 1260, 1200, 1120, 1023, 754, 692; ^1H NMR (250 MHz, CDCl_3) δ 1.96 (tt, $J = 7.5, 7.5$ Hz, 2H), 2.34 (t, $J = 7.5$ Hz, 2H), 2.64 (t, $J = 7.5$ Hz, 2H), 4.58 (s, 2H), 4.94 (s, 2H), 6.33 (s, 1H), 7.14–7.31 (m, 5H), 7.43 (s, 1H); ^{13}C NMR (125 MHz, CDCl_3) δ 26.4, 33.6, 35.1, 57.5, 57.6, 108.7, 121.3, 126.0, 128.4, 128.5, 141.3, 141.5, 154.9, 173.3; LRMS (EI, m/z) 274 (M^+), 257, 163; HRMS (EI, m/z) calcd for $\text{C}_{16}\text{H}_{18}\text{O}_4$, 274.1205; found, 274.1199.

To a solution of 2-formyl-3-(4-phenylbutanoyloxymethyl)furan (1.46 g, 5.35 mmol) in methanol–THF–acetic acid (30.8 mL, 20:20:1 v/v) was added NaBH_3CN (672 mg, 10.7 mmol) at 0 °C. The mixture was stirred for 18 h at room temperature, then poured into saturated aqueous sodium bicarbonate (10 mL) at 0 °C, and extracted with EtOAc. The organic layer was washed with water and brine, dried over anhydrous MgSO_4 , and concentrated in vacuo. The crude product was purified by silica gel column chromatography (3:1 hexane/EtOAc) to give **18** (1.21 g, 83%) as a colorless oil. IR (neat, cm^{-1}) 3450, 2940, 2853, 1740, 1600, 1500, 1450, 1260, 1200, 1120, 1023, 754, 692; ^1H NMR (250 MHz, CDCl_3) δ 1.84 (tt, $J = 7.5, 7.5$ Hz, 2H), 2.23 (t, $J = 7.5$ Hz, 2H), 2.52 (t, $J = 7.5$ Hz, 2H), 4.59 (s, 2H), 4.93 (s, 2H), 6.30 (d, $J = 1.8$ Hz, 1H), 7.04–7.26 (m, 5H), 7.27 (d, $J = 1.8$ Hz, 1H); ^{13}C NMR (125 MHz, CDCl_3) δ 26.3, 33.6, 35.0, 55.5, 57.5, 111.6, 117.0, 126.0, 128.4, 141.2, 142.2, 152.7, 174.0; LRMS (EI, m/z) 274 (M^+), 257, 163, 111. HRMS (EI, m/z) calcd for $\text{C}_{16}\text{H}_{18}\text{O}_4$, 274.1205; found, 274.1213.

2,4-Di(benzoyloxymethyl)furan (19). To a solution of **15** (273 mg, 1.18 mmol), Et_3N (328 μL , 2.36 mmol), and DMAP (14.2 mg, 0.12 mmol) in dry dichloromethane (6.8 mL) was added benzoyl chloride (181 μL , 1.29 mmol) at 0 °C, and the reaction mixture was stirred at room temperature for 1.5 h. After addition of 1 N HCl (2 mL), the resulting mixture was extracted with dichloromethane. The organic layer was washed with water and brine, dried over anhydrous MgSO_4 , and concentrated in vacuo. The crude product was purified by silica gel column chromatography (2:1 hexane/EtOAc) to give **19** (375 mg, 95%) as a pale yellow oil. IR (neat, cm^{-1}) 2950, 1720, 1610, 1460, 1280, 1100; ^1H NMR (250 MHz, CDCl_3) δ 5.14 (s, 2H), 5.21 (s, 2H), 6.53 (s, 1H), 7.32 (s, 1H), 7.33–7.45 (m, 4H), 7.48–7.61 (m, 2H), 7.92–7.96 (m, 4H); ^{13}C NMR (125 MHz, CDCl_3) δ 58.1, 58.4, 111.7, 121.5, 128.9, 129.7, 129.8, 129.8, 130.1, 130.6, 133.1, 133.1, 150.4, 162.3, 166.2, 166.4; LRMS (EI, m/z) 336 (M^+), 105. HRMS (EI, m/z) calcd for $\text{C}_{20}\text{H}_{16}\text{O}_5$, 336.0998; found, 336.1023.

2,3-Di(benzoyloxymethyl)furan (20). To a mixture of **16** (3.27 g, 14.1 mmol), Et_3N (3.92 mL, 28.2 mmol), and DMAP (172 mg, 1.41 mmol) in dry dichloromethane (30 mL) was added benzoyl chloride (2.45 mL, 21.2 mmol) at 0 °C, and the reaction mixture was stirred at

room temperature for 30 min. The solution was acidified with 1 N HCl (2 mL) and neutralized with saturated aqueous sodium bicarbonate. The resulting mixture was extracted with dichloromethane. The organic layer was washed with water and brine, dried over anhydrous MgSO_4 , and concentrated in vacuo. The crude product was purified by silica gel column chromatography (2:1 hexane/EtOAc) to give **20** (4.36 g, 92%) as a pale yellow solid. Mp 56–58 °C; IR (KBr, cm^{-1}) 2950, 1720, 1610, 1460, 1280, 1100; ^1H NMR (250 MHz, CDCl_3) δ 5.36 (s, 2H), 5.44 (s, 2H), 6.53 (d, $J = 1.8$ Hz, 1H), 7.38 (d, $J = 1.8$ Hz, 1H), 7.39–7.53 (m, 4H), 7.56–7.68 (m, 2H), 8.00–8.18 (m, 4H); ^{13}C NMR (125 MHz, CDCl_3) δ 56.7, 57.8, 112.0, 120.3, 128.9, 129.7, 129.8, 130.0, 130.6, 133.0, 133.1, 143.0, 147.9, 162.4, 166.2, 166.4; LRMS (EI, m/z) 336 (M^+), 105; HRMS (EI, m/z) calcd for $\text{C}_{20}\text{H}_{16}\text{O}_5$, 336.0993; found, 336.0992.

2-Benzoyloxymethyl-4-(4-phenylbutanoyloxymethyl)furan (21). To a solution of **17** (280 mg, 1.02 mmol), Et_3N (284 mL, 2.04 mmol), and DMAP (10.3 mg, 0.10 mmol) in dichloromethane (8 mL) was added benzoyl chloride (189 μL , 1.34 mmol) at 0 °C, and the mixture was stirred for 57 h at room temperature. The reaction was quenched with 1 N HCl (1 mL) at 0 °C and extracted with dichloromethane. The organic layer was washed with saturated aqueous sodium bicarbonate, water, and brine, dried over anhydrous MgSO_4 , and concentrated in vacuo. The crude product was purified by silica gel column chromatography (3:1 hexane/EtOAc) to give **21** (361 mg, 94%) as a colorless oil. IR (neat, cm^{-1}) 2820, 1720, 1600, 1500, 1450, 1270, 710; ^1H NMR (250 MHz, CDCl_3) δ 1.96 (tt, $J = 7.5, 7.5$ Hz, 2H), 2.35 (t, $J = 7.5$ Hz, 2H), 2.64 (t, $J = 7.5$ Hz, 2H), 4.96 (s, 2H), 5.27 (s, 2H), 6.51 (s, 1H), 7.14–7.47 (m, 9H), 8.03–8.06 (m, 2H); ^{13}C NMR (125 MHz, CDCl_3) δ 26.4, 33.5, 35.1, 57.5, 58.4, 111.6, 121.5, 126.0, 128.4, 128.4, 128.5, 129.6, 129.8, 133.1, 141.3, 142.1, 150.4, 166.2, 173.2; LRMS (CI, m/z) 379 ($\text{M}^+ + 1$), 163, 105. HRMS (EI, m/z) calcd for $\text{C}_{23}\text{H}_{22}\text{O}_5$, 378.1467; found, 378.1463.

2-Benzoyloxymethyl-3-(4-phenylbutanoyloxymethyl)furan (22). To a solution of 2-hydroxymethyl-3-(4-phenylbutanoyloxymethyl)furan **18** (1.02 g, 3.72 mmol), Et_3N (1.04 mL, 7.44 mmol), and DMAP (45.0 mg, 0.34 mmol) in dichloromethane (30 mL) was added benzoyl chloride (573 μL , 4.09 mmol) at 0 °C, and the mixture was stirred for 23 h at room temperature. The reaction was quenched with 1 N HCl (5 mL) at 0 °C and extracted with dichloromethane. The organic layer was washed with saturated aqueous sodium bicarbonate, water, and brine, dried over anhydrous MgSO_4 , and concentrated in vacuo. The crude product was purified by silica gel column chromatography (4:1 hexane/EtOAc) to give **22** (1.19 g, 95%) as a colorless oil. IR (neat, cm^{-1}) 2940, 2853, 1740, 1600, 1500, 1460, 1260, 1140, 1100, 940, 754, 792; ^1H NMR (250 MHz, CDCl_3) δ 1.93 (tt, $J = 7.5, 7.5$ Hz, 2H), 2.32 (t, $J = 7.5$ Hz, 2H), 2.61 (t, $J = 7.5$ Hz, 2H), 5.10 (s, 2H), 5.38 (s, 2H), 6.43 (d, $J = 1.8$ Hz, 1H), 7.12–7.55 (m, 9H), 8.01–8.05 (m, 2H); ^{13}C NMR (125 MHz, CDCl_3) δ 26.4, 33.5, 35.0, 56.5, 57.1, 111.8, 120.1, 126.0, 128.3, 128.3, 128.4, 129.7, 129.8, 133.1, 141.3, 143.0, 147.7, 166.1, 173.2. LRMS (CI, m/z) 379 ($\text{M}^+ + 1$), 257. HRMS (EI, m/z) calcd for $\text{C}_{23}\text{H}_{22}\text{O}_5$, 378.1467; found, 378.1423.

1,5-Dibenzoyloxymethyl-7-oxabicyclo[2.2.1]hept-5-ene-2,3-dicarboxylic Anhydride (23). A solution of **19** (355 mg, 1.06 mmol) and maleic anhydride (310 mg, 3.18 mmol) in toluene (2 mL) was stirred at room temperature for 12 h. After addition of further maleic anhydride (87.5 mg, 0.89 mmol), the reaction mixture was stirred at room temperature for 183 h. The solvent was evaporated under reduced pressure, and the crude compound was purified by silica gel column chromatography (4:1 hexane/EtOAc) to give **23** (297 mg, 64%) as a colorless oil. IR (neat, cm^{-1}) 3100, 2975, 1865, 1830, 1785, 1720, 1700, 1600, 1580, 1450, 1270, 1120, 710, 680; ^1H NMR (400 MHz, CDCl_3) δ 3.36 (d, $J = 6.8$ Hz, 1H), 3.57 (d, $J = 6.8$ Hz, 1H), 4.79 (d, $J = 13.0$ Hz, 1H), 5.03 (d, $J = 1.7$ Hz, 2H), 5.16 (d, $J = 13.0$ Hz, 1H), 5.47 (s, 1H), 6.42 (d, $J = 1.7$ Hz, 1H), 7.43–7.49 (m, 4H), 7.59–7.61 (m, 2H), 8.01–8.07 (m, 4H); ^{13}C NMR (125 MHz, CDCl_3) δ 50.7, 51.1,

59.3, 61.0, 82.8, 91.8, 128.5, 128.6, 129.0, 129.2, 129.7, 129.8, 133.1, 133.4, 133.6, 148.2, 165.9, 166.0, 167.8, 169.3; LRMS (EI, m/z) 337, 307, 105.

1,5-Dibenzoyloxymethyl-7-oxabicyclo[2.2.1]heptane-2,3-dicarboxylic Anhydride (9). To a solution of **23** (83.2 mg, 1.91 mmol) in Et₂O (2 mL) and THF (1 mL) was added 5% Rh/Al₂O₃ (15 mg). The reaction mixture was stirred at room temperature under a hydrogen atmosphere, filtered through Celite, and concentrated in vacuo. The oily crude product was taken up in hexanes–EtOAc (2 mL 5:1 v/v) to afford a precipitate of a white solid. This product was purified by gel permeation chromatography to give **9** (21.8 mg, 26%) as colorless crystals. Mp 149–152 °C; IR (KBr, cm⁻¹) 2970, 1865, 1830, 1785, 1720, 1600, 1580, 1450, 1270, 1120, 710; ¹H NMR (500 MHz, CDCl₃) δ 1.47 (dd, $J = 12.4, 5.5$ Hz, 1H), 2.28 (ddd, $J = 12.4, 12.4, 5.5$ Hz, 1H), 2.93–2.96 (m, 1H), 3.33 (d, $J = 7.5$ Hz, 1H), 3.78 (d, $J = 7.5$ Hz, 1H), 4.26 (dd, $J = 11.8, 9.4$ Hz, 1H), 4.52 (dd, $J = 11.8, 5.8$ Hz, 1H), 4.89 (d, $J = 12.8$ Hz, 1H), 4.95 (d, $J = 12.8$ Hz, 1H), 5.10 (d, $J = 4.9$ Hz, 1H), 7.45–7.50 (m, 4H), 7.60–7.62 (m, 2H), 8.02–8.06 (m, 4H); ¹³C NMR (125 MHz, CDCl₃) δ 33.6, 39.7, 46.5, 50.6, 61.2, 62.5, 80.8, 87.2, 127.5, 127.7, 128.2, 128.2, 128.6, 128.9, 132.4, 132.6, 164.7, 165.2, 167.7, 170.1; LRMS (CI, m/z) 437 (M⁺ + 1), 315, 123, 105. Anal. Calcd for C₂₄H₂₀O₈: C, 66.05; H, 4.62. Found: C, 65.82; H, 4.69.

1,6-Dibenzoyloxymethyl-7-oxabicyclo[2.2.1]hept-5-ene-2,3-dicarboxylic Anhydride (24). A solution of **20** (370 mg, 1.10 mmol) and maleic anhydride (324 mg, 3.30 mmol) in toluene (2 mL) was stirred at room temperature for 68 h. After addition of further maleic anhydride (108 mg, 1.10 mmol), the reaction mixture was stirred at room temperature for 216 h. The solvent was evaporated under reduced pressure, and the crude compound was purified by silica gel column chromatography (4:1 hexane/EtOAc) to give **24** (305 mg, 63%) as a colorless oil. IR (neat, cm⁻¹) 2820, 1865, 1830, 1720, 1705, 1600, 1580, 1450, 1270, 1120, 710; ¹H NMR (250 MHz, CDCl₃) δ 3.41 (d, $J = 6.9$ Hz, 1H), 3.55 (d, $J = 6.9$ Hz, 1H), 5.05 (m, 4H), 5.48 (d, $J = 2.0$ Hz, 1H), 6.54 (d, $J = 2.0$ Hz, 1H), 7.40–7.48 (m, 4H), 7.55–7.63 (m, 2H), 7.96–8.03 (m, 4H); ¹³C NMR (125 MHz, CDCl₃) δ 49.7, 52.3, 59.1, 60.7, 82.1, 91.0, 128.6, 128.7, 129.0, 129.1, 129.6, 129.8, 133.5, 133.7, 134.5, 146.9, 165.5, 165.9, 167.8, 169.1; LRMS (EI, m/z) 337, 307.

1,6-Dibenzoyloxymethyl-7-oxabicyclo[2.2.1]heptane-2,3-dicarboxylic Anhydride (10). To a solution of **24** (94.4 mg, 220 μmol) in THF (1.5 mL) was added 5% Rh/Al₂O₃ (10 mg), and the mixture was stirred at room temperature under a hydrogen atmosphere. The reaction mixture was filtered through Celite and concentrated in vacuo. The oily crude product was taken up in 2 mL of hexane/EtOAc (4:1) to afford a precipitate of **10** (78.3 mg, 83%) as a colorless solid. Mp 75–78 °C; IR (KBr, cm⁻¹) 2820, 1865, 1830, 1785, 1720, 1600, 1580, 1450, 1270, 1120, 755, 710, 680; ¹H NMR (500 MHz, CDCl₃) δ 1.47 (dd, $J = 12.4, 5.5$ Hz, 1H), 2.89 (ddd, $J = 12.4, 12.4, 5.5$ Hz, 1H), 2.95–2.99 (m, 1H), 3.39 (d, $J = 7.5$ Hz, 1H), 3.67 (1H, d, $J = 7.5$ Hz, 1H), 4.29 (dd, $J = 12.0, 9.3$ Hz, 1H), 4.61 (dd, $J = 12.0, 5.5$ Hz, 1H), 4.87 (d, $J = 13.0$ Hz, 1H), 4.95 (d, $J = 13.0$ Hz, 1H), 5.04 (d, $J = 5.5$ Hz, 1H), 7.40–7.47 (m, 4H), 7.54–7.61 (m, 2H), 7.95–8.02 (m, 4H); ¹³C NMR (125 MHz, CDCl₃) δ 32.8, 40.6, 47.2, 51.9, 62.0, 63.5, 79.8, 89.5, 128.5, 128.7, 129.0, 129.2, 129.5, 129.7, 133.3, 133.6, 165.6, 166.1, 169.4, 170.5; LRMS (EI, m/z) 436 (M⁺) 315, 122, 105. HRMS (EI, m/z) calcd for C₂₄H₂₀O₈, 436.1158; found, 436.1140.

1-Benzoyloxymethyl-5-(4-phenylbutanoyloxymethyl)-7-oxabicyclo[2.2.1]hept-5-ene-2,3-dicarboxylic Anhydride (25). A solution of **21** (350 mg, 0.93 mmol) and maleic anhydride (272 mg, 2.78 mmol) in toluene (0.5 mL) was stirred at room temperature for 17 h. After further addition of maleic anhydride (90.7 mg, 0.93 mmol) and toluene (0.5 mL), the reaction mixture was stirred at room temperature for 72 h. The solvent was evaporated under reduced pressure, and the crude product was purified by silica gel column chromatography (3:1 hexane/EtOAc) to give **25** (297.2 mg, 68%) as a colorless oil. IR (neat, cm⁻¹)

3100, 2950, 1865, 1780, 1730, 1600, 1500, 1450, 1270, 920, 710; ¹H NMR (250 MHz, CDCl₃) δ 1.97 (tt, $J = 7.5, 7.5$ Hz, 2H), 2.37 (t, $J = 7.5$ Hz, 2H), 2.66 (t, $J = 7.5$ Hz, 2H), 3.32 (d, $J = 7.0$ Hz, 1H), 3.46 (d, $J = 7.0$ Hz, 1H), 4.75 (s, 2H), 4.77 (d, $J = 12.8$ Hz, 1H), 5.16 (d, $J = 12.8$ Hz, 1H), 5.36 (s, 1H), 6.33 (s, 1H), 7.15–7.59 (m, 8H), 8.02–8.06 (m, 2H); ¹³C NMR (125 MHz, CDCl₃) δ 26.2, 33.2, 35.0, 50.7, 51.0, 58.8, 61.0, 82.7, 91.7, 126.0, 128.4, 128.5, 129.2, 129.8, 132.9, 133.5, 140.9, 165.8, 167.7, 169.3, 172.9; LRMS (EI, m/z) 378, 163, 105.

1-Benzoyloxymethyl-5-(4-phenylbutanoyloxymethyl)-7-oxabicyclo[2.2.1]heptane-2,3-dicarboxylic Anhydride (11). To a solution of **25** (200 mg, 0.42 mmol) in Et₂O (2 mL) and THF (2 mL) was added 5% Rh/Al₂O₃ (15 mg). The reaction mixture was stirred at room temperature under a hydrogen atmosphere, filtered through Celite, and concentrated in vacuo to give **11** (125 mg, 62%) as a white solid. Mp 100–103 °C; IR (KBr, cm⁻¹) 2950, 1865, 1780, 1730, 1600, 1500, 1450, 1270, 1100, 980, 920, 760, 710; ¹H NMR (250 MHz, CDCl₃) δ 1.34 (dd, $J = 12.5, 5$ Hz, 1H), 1.92 (tt, $J = 7.5, 7.5$ Hz, 2H), 2.24–2.37 (m, 3H), 2.63 (t, $J = 7.5$ Hz, 2H), 2.70–2.79 (m, 1H), 3.30 (1H, d, $J = 7.5$ Hz), 3.54 (d, $J = 7.5$ Hz, 1H), 3.97 (dd, $J = 12.5, 7.5$ Hz, 1H), 4.34 (dd, $J = 12.5, 7.5$ Hz, 1H), 4.77 (d, $J = 12.0$ Hz, 1H), 4.95 (d, $J = 12.0$ Hz, 1H), 5.00 (d, $J = 5.0$ Hz, 1H), 7.12–7.30 (m, 5H), 7.42–7.48 (m, 2H), 7.55–7.58 (m, 1H), 8.00–8.03 (m, 2H); ¹³C NMR (125 MHz, CDCl₃) δ 26.1, 32.8, 33.3, 34.9, 40.3, 47.1, 51.8, 61.9, 62.8, 79.7, 89.1, 126.1, 128.4, 128.5, 129.3, 129.7, 133.4, 141.0, 146.8, 165.5, 169.4, 170.4, 172.9; LRMS (EI, m/z) 478, 315, 147, 105. HRMS (EI, m/z) calcd for C₂₇H₂₆O₈, 478.1628; found, 478.1641.

1-Benzoyloxymethyl-6-(4-phenylbutanoyloxymethyl)-7-oxabicyclo[2.2.1]hept-5-ene-2,3-dicarboxylic Anhydride (26). A solution of **22** (487 mg, 1.29 mmol) and maleic anhydride (379 mg, 3.86 mmol) in toluene (2 mL) was stirred at room temperature for 136 h. The solvent was evaporated under reduced pressure, and the crude compound was purified by silica gel column chromatography (7:2 hexane/EtOAc) to give **26** (314 mg, 51%) as a colorless oil. IR (neat, cm⁻¹) 2950, 1865, 1780, 1730, 1600, 1500, 1450, 1270, 1100, 920, 710; ¹H NMR (250 MHz, CDCl₃) δ 1.92 (tt, $J = 7.5, 7.5$ Hz, 2H), 2.32 (t, $J = 7.5$ Hz, 2H), 2.62 (t, $J = 7.5$ Hz, 2H), 3.37 (d, $J = 7.0$ Hz, 1H), 3.43 (d, $J = 7.0$ Hz, 1H), 4.79 (s, 2H), 4.98 (s, 2H), 5.45 (d, $J = 1.75$ Hz, 1H), 6.45 (d, $J = 1.75$ Hz, 1H), 7.13–7.59 (m, 8H), 7.98–8.02 (m, 2H); ¹³C NMR (125 MHz, CDCl₃) δ 33.2, 35.0, 49.6, 52.3, 58.6, 60.6, 82.0, 90.9, 126.2, 128.4, 128.5, 128.6, 129.1, 129.7, 133.5, 134.5, 140.9, 146.8, 165.4, 167.8, 169.1, 172.8; LRMS (EI, m/z) 379, 105.

1-Benzoyloxymethyl-6-(4-phenylbutanoyloxymethyl)-7-oxabicyclo[2.2.1]heptane-2,3-dicarboxylic Anhydride (12). To a solution of **26** (249 mg, 0.52 mmol) in Et₂O (3 mL) and THF (3 mL) was added 5% Rh/Al₂O₃ (15 mg). The reaction mixture was stirred at room temperature under a hydrogen atmosphere, filtered through Celite, and concentrated in vacuo to give **12** (250 mg, quant.) as colorless crystals. Mp 91–93 °C; IR (KBr, cm⁻¹) 2950, 1865, 1780, 1730, 1600, 1500, 1450, 1270, 1100, 980, 920, 760, 710; ¹H NMR (250 MHz, CDCl₃) δ 1.34 (dd, $J = 12.5, 5.0$ Hz, 1H), 1.92 (tt, $J = 7.5, 7.5$ Hz, 2H), 2.24–2.37 (m, 3H), 2.63 (t, $J = 7.5$ Hz, 2H), 2.70–2.79 (m, 1H), 3.30 (d, $J = 7.5$ Hz, 1H), 3.54 (d, $J = 7.5$ Hz, 1H), 3.97 (dd, $J = 12.5, 7.5$ Hz, 1H), 4.34 (dd, $J = 12.5, 7.5$ Hz, 1H), 4.77 (d, $J = 12$ Hz, 1H), 4.95 (d, $J = 12$ Hz, 1H), 5.00 (d, $J = 5.0$ Hz, 1H), 7.12–7.30 (m, 5H), 7.42–7.48 (m, 2H), 7.55–7.58 (m, 1H), 8.00–8.03 (m, 2H); ¹³C NMR (125 MHz, CDCl₃) δ 26.1, 32.8, 33.3, 34.9, 40.3, 47.1, 51.8, 61.9, 62.8, 79.7, 89.1, 126.1, 128.4, 128.5, 129.3, 129.7, 133.4, 141.0, 146.8, 165.5, 169.4, 170.4, 172.9; LRMS (EI, m/z) 478, 315, 147, 105. HRMS (EI, m/z) calcd for C₂₇H₂₆O₈, 478.1628; found, 478.1641.

Construction of the Binding Model. To construct a binding model of norcantharidin carboxylate and the catalytic site of PP2B, a computational docking study was performed based on the reported PP2B–FKBP–FK506 complex structure (pdb code, 1TCO). The preliminary binding model was constructed in the Affinity module of the Insight II molecular modeling program developed by MSI (now

succeeded by Accelrys, San Diego). Affinity is a program for automatically docking a ligand to a receptor using a combination of Monte Carlo type and simulated annealing procedures. The molecular mechanics program employed in Affinity is the Discover 3 module in conjunction with the force fields supported by that program. In the first orientation, we constructed a "grid" which is partitioned into bulk (nonflexible) and movable atoms at the ligand/receptor system; interactions among bulk atoms are approximated by using the accurate and efficient molecular mechanical/grid (MM/Grid) method, while interactions among movable atoms are treated using a full force field representation. The grid was defined by the amino acid residues within 6 Å around the phosphate ion, including in the catalytic site of PP2B. The initial placements of norcantharidin within the PP2B catalytic site were made using a Monte Carlo type procedure to search both conformational and Cartesian space. Second, a simulated annealing phase optimized each ligand placement. The structures were then subjected to energy minimization based on molecular dynamics.

Protein Phosphatase Inhibition Assays. Phosphatases PP1 (rabbit skeletal muscle), PP2A (rabbit skeletal muscle, composed of α , β and catalytic subunit), and PP2B (bovine brain) were purchased from UBI (Upstate Biotechnology Inc.). PTP1B was purchased from BIOMOL (BIOMOL Research Laboratories Inc). Cyclophilin A (calf thymus) and cyclosporin A were purchased from SIGMA and CALBIOCHEM, respectively. Protein phosphatase assays were carried out according to the UBI protocol in the presence or absence of the appropriate concentration of a cantharidin derivative. For PP1 and PP2A assays, the Ser/Thr Phosphatase Assay Kit 1 (UBI) was used, in which free phosphate ion released from a substrate phosphopeptide (KRpTIRR) is quantified by colorimetric analysis (630 nm) using the Malachite Green method (enzyme concentrations: 4 units/mL PP1; 56 nM PP2A).

For PP2B inhibition assays shown in the Figure 7C, RII phosphopeptide (DLDVPIPIGRFDRRVpSVAAE, BIOMOL)¹⁸ was used as a substrate. Briefly, the phosphopeptide (90 μ M) was incubated with PP2B (230 nM) at 37 °C (in 40 mM Tris·HCl buffer pH 7.5, 0.1 M KCl, 6 mM MgCl₂, 0.1 mM CaCl₂, 0.1 mg/mL BSA, 0.05 mM DTT, 0.25 μ M calmodulin) in the absence or presence of inhibitors. For evaluation of the cyclosporin A–cyclophilin A complex, concentration of cyclophilin A was varied in the presence of 10 μ M cyclosporin A. *p*-Nitrophenyl phosphate (pNPP) was used as a substrate for the other preliminary PP2B assays (in 50 mM Tris·HCl buffer pH 7.0, 0.1 mM CaCl₂, 2.5 mM NiCl₂, 0.3 mg/mL BSA, 0.25 μ M calmodulin, 2.4 mM pNPP, 57 nM PP2B) and PTP1B assays (in 50 mM Hepes buffer pH 7.2, 50 mM NaCl, 1.0 mM EDTA, 1.0 mM DTT, 1.0 mg/mL BSA, 8.0 nM PTP1B). Hydrolysis of the substrate was followed in terms of the absorption of the hydrolysis product, *p*-nitrophenol (415 nm).

Acknowledgment. This work was supported in part by grants from The Naito Foundation, Suzuken Memorial Foundation, and Hoh-ansha Foundation and by a Grant-in-Aid for Creative Scientific Research (No. 13NP0401) and a Grant-in-Aid for Scientific Research from the Japan Society for the Promotion of Science, a Grant-in-Aid for Scientific Research on Priority Areas (A), and a Grant-in-Aid for the COE project, Giant Molecules and Complex Systems, from The Ministry of Education, Culture, Sports, Science and Technology, as well as the Chugai Pharmaceutical Award in Synthetic Organic Chemistry.

JA034694Y